Impact of ferroelectric and superparaelectric nanoparticles on phase transitions and dynamics in nematic liquid crystals

Szymon Starzonek,* Sylwester J. Rzoska, and Aleksandra Drozd-Rzoska
Institute of High Pressure Physics of Polish Academy of Sciences, ulica Sokołowska 29/37, 01-142 Warsaw, Poland

Krzysztof Czupryński
Military University of Technology, Institute of Chemistry, ulica Kaliskiego 2, 00-908 Warsaw, Poland

Samo Kralj
Condensed Matter Physics Department, Jozef Stefan Institute, Jamova 39, 1000 Ljubljana, Slovenia
and Faculty of Natural Sciences and Mathematics, University of Maribor, Koroska 160, 2000 Maribor, Slovenia
(Received 4 March 2017; published 9 August 2017)

Results of broadband dielectric spectroscopy (BDS) studies of pure liquid crystalline (4-pentyloxy-4-biphenylcarbonitryle) 5OCB and its nanocolloids with $BaTiO_3$ nanoparticles (NPs) under varying pressure and temperature are presented. The notable impact of NPs on phase transitions and dynamics was found. Particularly strong impact on pretransitional behavior was observed for relatively low concentrations of NPs, which can be related to the NPs-induced disorder. There are also notable differences between pressure and temperature paths of studies for nanocomposites, absent for the pure LC compound. For instance, tests focused on the translational orientational decoupling via the fractional Debye-Stokes-Einstein relation yielded $S = 0.71$ and $S = 0.3$ for the temperature and pressure paths, respectively: $S = 1$ is for the complete coupling. The possible theoretical frame of observed phenomena is also proposed.

DOI: 10.1103/PhysRevE.96.022705

I. INTRODUCTION

In the last decade, hybrid composites of liquid crystals (LCs) and nanoparticles (NPs) have become a much-studied topic in soft-matter and liquid-crystal physics [1–4]. This is associated with their extraordinary metamaterial features resulting from the mutually beneficial combination of unique semiordered fluids and solid nanoparticles. Nanoparticles can influence the local mesophase order in liquid crystals and, similarly, the LC matrix can facilitate NPs arrangements [5–7]. This is supplemented by a set of specific features related to material origins of NPs: metallic, semiconductor, or dielectric. All these can create from LC + NP hybrid composites an exceptional kind of system for new generations of optoelectronic devices [8,9]. However, the fundamental evidence regarding phase transitions is still surprisingly limited, despite the fact that adding nanoparticles can notably change the LC host system, leading to the emergence of new meta-LC systems. Nanoparticles can act as the moderator of local molecular properties of the liquid crystalline host [4–7]. On the other hand, the local field or geometrical hindrances associated with NPs could influence the local LC symmetry, leading to the shift of phase-transition temperatures or the decrease of the switching voltage of structural transformations [5]. For the physics of liquid crystals, particularly important are forms and impacts of pretransitional effects, their metrics, and the exceptional complex dynamics [10]. However, evidence related to these issues for LCs + NPs composites is still very limited. In fact, the first experimental results focusing on critical exponents, the range of critical effects, and the value of the discontinuity for weakly discontinuous phase transitions have been reported only recently [1,4]. This was the case of dielectric constant behavior in the $BaTiO_3$ nanoparticle (nonferroelectric) dodecylcyanobiphenyl (12CB, isotropic smectic-*A* solid mesomorphism) nanocolloid [1]. This reports presents broadband dielectric spectroscopy (BDS) results for 4-pentyloxy-4-biphenylcarbonitrile (5OCB) + $BaTiO_3$ nanoparticles (both ferroelectric and nonferroelectric), yielding insight into dielectric constant and dynamics. Results are for both the temperature and the pressure path. It is worth recalling that cooling or heating changes the activation energy, whereas compressing influences mainly the free volume changes.

II. EXPERIMENT

5OCB belongs to the group of the most "classical" LC compounds, regarding both fundamentals and applications in displays technology. It is characterized by the following mesomorphism: isotropic (*I*), 341 K; nematic (*N*), 326 K; crystal. 5OCB has a strong dipole moment (ca. 4D) at one of the termini of the molecule and approximately parallel to its long axis; therefore, no additional orientation of the sample is required. The high-purity sample was synthesized at Warsaw Military Technical University (Poland). $BaTiO_3$ NPs were purchased from Research Nanomaterials (USA). All of the $BaTiO_3$ phases exhibit ferroelectricity except the cubic phase: This research is associated with the paraelectric cubic phase NPs ($2r = 50$ nm) and ferroelectric tetragonal phase ($2r = 200$ nm).

LC samples were degassed immediately prior to measurements. Measurements were carried out using the broadband dielectric spectrometer (BDS) Novocontrol, supported by the Quattro temperature controlling system. This enabled

*starzoneks@unipress.waw.pl

five-digits resolution in dielectric measurements and $\Delta T = +0.02$ K temperature stabilization. Mixtures of 5OCB and NPs were sonicated with frequency $f = 42$ kHz for a few hours in the isotropic phase until obtaining the homogenous mixture for testing. No sedimentation for at least 24 hr was observed; hence, the final colloid did not contain any additional stabilizing agent. Samples were placed in the measurement capacitor made from Invar, with $d = 0.2$ mm gap and diameter $2r = 20$ mm. The quartz ring was used as the spacer. This enables observation of the interior of the capacitor. The latter and the macroscopic gap of the capacitor made it possible to avoid bubbles, distorting results. For each concentration of nanoparticles at least three series of measurements were carried out.

Measurements of the dielectric permittivity $\varepsilon^*(f) = \varepsilon'(f) - \varepsilon''(f)$ were performed using and impedance Alpha-A analyzer by Novocontrol over a frequency range 1–10^6 Hz. For the isobaric (atmospheric pressure) experiment a temperature range was obtained: 373 K–273 K. The temperature was controlled and stabilized by the Quatro cryosystem (Novocontrol) using liquid nitrogen with stability better than $\Delta T = 0.02$ K. The temperature step was $dT = 1$ K. For the isothermal ($T = 368$ K) measurements the same impedance analyzer was used. A pressure range for studied samples was from 0.1 to 400 MPa, with a step $dP = 1.25$ MPa. The temperature was stabilized using a thermostatic set (Julabo); the stability was performed better than $\Delta T = 0.02$ K. The high-pressure set is shown in Ref. [11]: Pressure was monitored via two tensometric meters and temperature via the copper-constantan thermocouple within the pressure chamber.

All data were fitted using the Havriliak-Negami function $\varepsilon^*(\omega) = \varepsilon_\infty + \frac{\Delta\varepsilon}{[(1+i\omega\tau)^\alpha]^\beta} + (\frac{\sigma_{DC}}{\varepsilon_0\omega})^S$. The dielectric constant (static permittivity, ε_s) was obtained as a value of the plateau part appeared for the real part of a dielectric permittivity as a function of temperature taken at a characteristic for LC samples frequency $f = 100$ kHz. The DC conductivity (σ_{DC}) was estimated ε'' as a low-frequency part with a slope $S = -1$ from the loss spectra.

III. RESULTS AND DISCUSSION

The evolution of a dielectric constant enables getting insight into the dominant way of dipole-dipole arrangement in the given system. For the predominantly parallel ordering, the value of dielectric constant decreases with rising temperature. When the antiparallel collocation prevails, dielectric constant decreases on cooling [12–15]. Such behavior occurs for pretransitional effects in the isotropic phase of 5OCB + NPs ($BaTiO_3$) nanocolloid (Fig. 1). The change of $\varepsilon(T)$ behavior on approaching the mesophase is caused by the increasing number of 5OCB molecules within prenematic fluctuations, for which the equivalence of $\vec{n}$ and $-\vec{n}$ directors is the key feature [5–7]. In each tested case the pretransitional effect can be well portrayed by the same dependence as in "pure" LC [11–13],

$$\varepsilon(T) = \varepsilon^* + a(T - T^*) + A(T - T^*)^\phi, \quad T > T_{IM}, \quad (1)$$

where $T^* = T_{IM} - \Delta T$ is the extrapolated temperature of the continuous phase transition, ΔT is the measure of the discontinuity of the isotropic LC mesophase transition, and the exponent $\phi = 1 - \alpha$, α is the exponent of the specific heat. T_{IM} is the isotropic LC mesophase discontinuous phase transition temperature (clearing temperature).

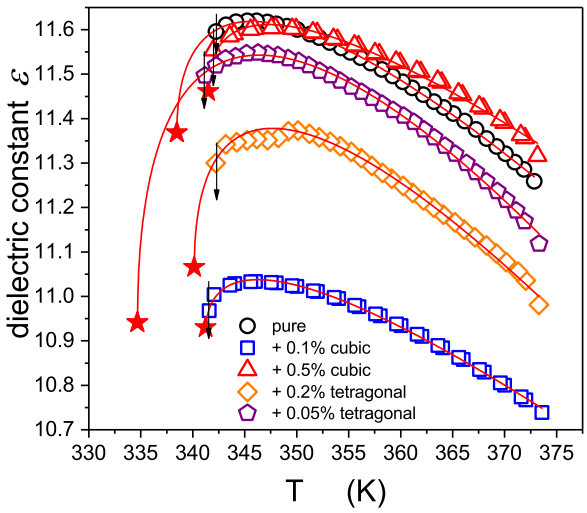

FIG. 1. The temperature evolution of dielectric constant in pure and $BaTiO_3$ doped liquid crystalline 5OCB (isotropic phase). The red stars denote the extrapolated continuous phase transition temperature and the black arrow the "real" discontinuous phase transition. The distance between stars and arrows shows the value of the discontinuity of the isotropic mesophase transition.

The parallel of such behavior was reported for the pressure path of approaching the mesophase (nematic, smectic) [4,12],

$$\varepsilon(T) = \varepsilon^* + b(P^* - P) + B(P^* - P)^\phi, \quad P < P_{IM}, \quad (2)$$

where $P^* = P_{IM} + \Delta P$ is the extrapolated temperature of the continuous phase transition, ΔP is the pressure metric of the discontinuity of the isotropic LC mesophase transition, and the exponent $\phi = 1 - \alpha$, α is the exponent of the specific heat. The addition of NPs seems to have no impact on the form of parametrization of the pretransitional effects (Fig. 1 and Table I), but it has the strong influence on the total value of dielectric constant and the discontinuity of the transitions. Adding the small amount of NPs ($x \approx 0.5\%$) decreases dielectric constant, but for higher concentrations the value of dielectric constant notably increase. One can speculate that for very small amounts of NPs the local arrangement of 5OCB is distorted, but when increasing the amount of NPs it seems to be strengthened. It is notable that the concentration of NPs has a very strong impact on ΔT, as visible in Fig. 1 and Table I: In fact, for the concentration ($x \approx 0.5\%$) of NPs the phase transition approaches the continuous pattern. Note that similar nonmonotonic temperature behavior has been observed [16–18] in mixtures of different LCs and aerosol NPs. Such behavior is expected when a kind of quenched random field-type disorder is present, which is presented in more detail in the Appendix.

Note that small nanoparticles in the paraelectric cubic phase with its diameter $d = 50$ nm has the same impact as the tetragonal phase one. This effect can be explained using the superparaelectricity theory. For nanoparticles in the cubic phase with a size below its charge correlation length the permanent dipole moment can be induced [19].

TABLE I. Parameters describing pretransitional effects in 5OCB + $BaTiO_3$ NPs nanocolloids in Fig. 1 via Eq. (1).

Sample	NPs size/Phase	T^C (K)	ε^*	T^* (K)	a	A	α
5OCB		342.23_5	11.36_9	338.47_3	-0.034_7	0.185_3	0.5
5OCB + 0.1% NPs	50 nm/cubic	341.57_1	10.93_0	341.25_0	-0.024_3	0.108_8	0.5
5OCB + 0.5% NPs	50 nm cubic	341.97_5	11.42_0	341.47_9	-0.025_8	0.124_4	0.5
5OCB + 0.05% NPs	200 nm/tetragonal	341.16_7	10.94_1	334.67_8	-0.051_5	0.351_9	0.5
5OCB + 0.2% NPs	200 nm tetragonal	342.07_0	11.06_6	340.14_6	-0.041_6	0.227_9	0.5

It yields a ferroelectric effect even without tetragonal phase, which explains the same behavior and influence of the small ($d = 50$ nm) cubic and the large ($d = 200$ nm) tetragonal nanoparticles.

In the nematic phase the nonoriented sample was monitored, a predominantly spontaneous parallel arrangement of permanent dipole moment coupled with 5OCB molecules was detected: It was notably weaker for the highest tested concentration of NPs (Fig. 2). When compressing finally the solid phase is reached: There is some impact of nanoparticles here, but much weaker than in the fluid phase [4]. Finally, it is notable that for the temperature scan (Fig. 1) the impact of pressure on the clearing temperature is almost negligible. For the pressure scan the clearing pressure notably decreases with rising concentration of NPs. The question arises if the notable difference for the temperature and pressure behavior can be related to the fact that on compressing nanoparticles can have a preferable locations, associated with free volume gaps [4,11–15].

Subsequent results reported below focus on dynamic issues, namely the evolution of dielectric relaxation time and the decoupling between translational and orientational degrees of freedom. The primary relaxation times are determined from peak frequencies as dielectric loss curves, which examples are shown in the inset in Fig. 2 as $\tau = (2\pi f_{\text{peak}})^{-1}$ [4,20,21]. One can see that the inset in Fig. 2 shows that the addition of $BaTiO_3$ has very weak impact on the distribution of relaxation times, which metrics are slopes of lines, in the $\log_{10}\varepsilon$ vs $\log_{10} f$ plot, for $f > f_{\text{peak}}$ and $f < f_{\text{peak}}$. However, there are other unique features induced by adding NPs: (i) An additional relaxation process in the low-frequency region dominated by conductivity emerges; (ii) the range of the region where $\log_{10}\varepsilon/\log_{10} f = \text{const}$ for $f < f_{\text{peak}}$ increases from 2 decades (5OCB) to 3 decades (5OCB + 0.5% NPs); (iii) adding of NPs decreases by ca. a decade the values of $\varepsilon_{\text{peak}}''$, which is the rough metric of the energy associated with the reorientation of dipoles. For the low-frequency region where $\varepsilon''(f) \propto 1/f$ is the distance between 5OCB and 5OCB + NPs the case can differ even by 2 decades, which suggests a similar distance between relaxation times associated with translational process [22]. The last comment indicated the comparison of translational and orientational process, which for "classical" systems are expressed via Debye-Stokes-Einstein (DSE) or its fractional counterpart, namely,

$$\sigma(T,P)[\tau(T,P)]^S = \text{const}, \tag{3}$$

where $\sigma = \sigma_{DC} = 2\pi f \varepsilon_0 \varepsilon''$ for the low-frequency part of the spectra presented in the inset in Fig. 2. The DSE relations ($S = 1$, translational orientational coupling) convert into the fractional Debye-Stokes-Einstein (FDSE) relation for $S \neq 1$ [4,20,22]. Results of such analysis, in the nematic and nematic-doped mesophase are shown in Fig. 3. For "pure" 5OCB there is a very strong decoupling, which can be associated with predominantly parallel ordering of rodlike 5OCB molecules.

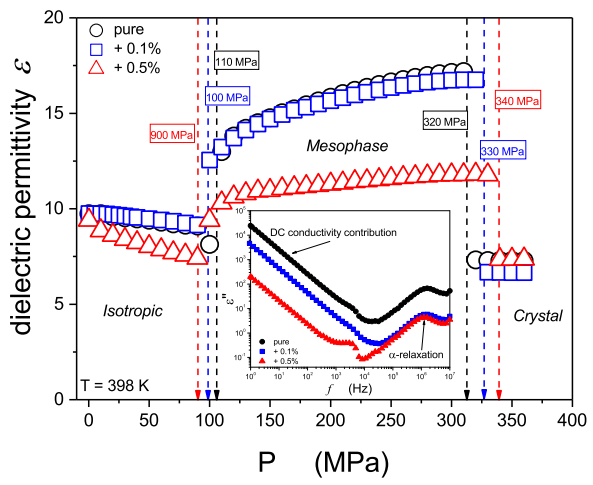

FIG. 2. The isothermal ($T = 368$ K) pressure evolution of dielectric constant in 5OCB and 5OCB + NPs ($BaTiO_3$, superparaelectric cubic phase) systems. The inset shows the example of dielectric loss spectra for $P = 250$ MPa in mesophase.1

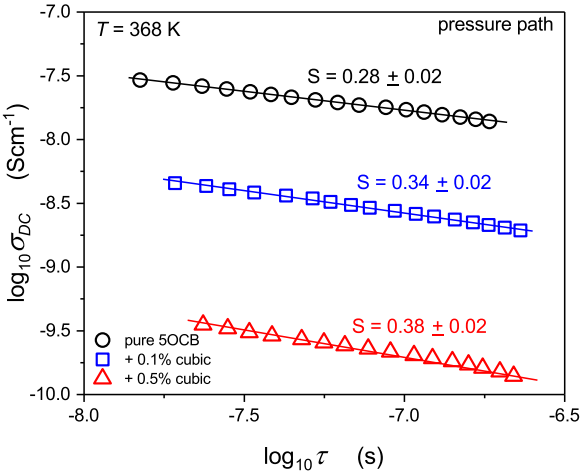

FIG. 3. A plot focused on the translational-orientational coupling ($S = 1$) and decoupling ($S < 1$) via FDSE Eq. (1): the behavior in the nematic and nematic NP-doped mesophases and the pressure path. For the temperature scan the S parameter equals 0.71 in pure liquid crystal.

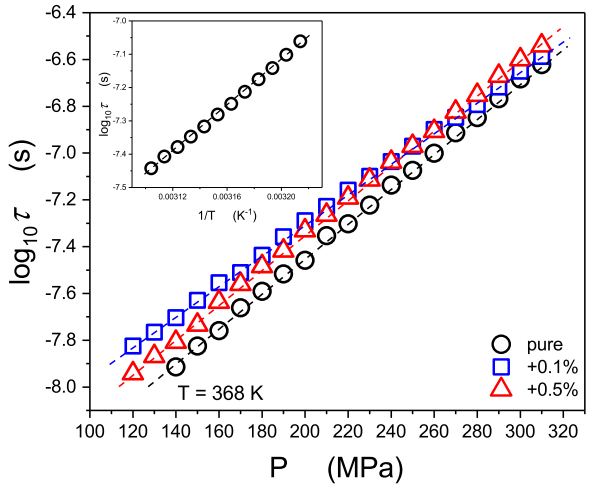

FIG. 4. The pressure behavior dependence of dielectric relaxation times in 5OCB and 5OCB + NPs ($BaTO_3$) nanocolloids. The inset presents the Arrhenius plot showing the behavior of the temperature evolution of the primary dielectric relaxation time, pure 5OCB.

This decoupling notably weakens when adding nanoparticles, which can be associated with distorting of the parallel arrangement of 5OCB molecules by nanoparticles. Similar test focused on the validity of the DSE/FDSE behavior, but for the temperature scan under atmospheric pressure. The most striking feature is not only the occurrence of the FDSE behavior also in this case, but the fact that the translational orientational decoupling is twice as strong for the temperature scan than for the pressure scan. This suggest that for clearly rodlike molecules the general relation (3) valid for low-molecular-weight liquids (like glycerol, for instances) should be in the given case replaced by two dependencies [22]:

$$\sigma(T)[\tau(T)]^{S_T} = \text{const} \quad \text{and} \quad \sigma(P)[\tau(P)]^{S_P} = \text{const}. \quad (4)$$

All the above also may indicate that for rodlike molecules compressing promotes the parallel ordering of rodlike molecules. Figure 4 shows the temperature (a) and pressure (b) evolution of primary relaxation times. The applied scale shows the clear validity of the simple Arrhenius behavior,

$$\tau(T) = \tau_0 \exp\left(\frac{\Delta E_a}{RT}\right), \quad \text{for} \quad P = \text{const}, \quad (5)$$

and its pressure counterpart, the Barus dependence,

$$\tau(P) = \tau_0 \exp\left(\frac{P\Delta V_a}{RT}\right), \quad \text{for} \quad T = \text{const}, \quad (6)$$

where ΔE_a and ΔV_a stand for the activation energy and volume, respectively. The value of the activation energy ΔE_a for pure liquid crystal averages ca. 68 kJ mol^{-1}. For the other samples calculating this value was not possible because the dielectric relaxation peaks occur in high-frequency region. The high-pressure study give values of activation volume—$\Delta V_a = 9.32\ \text{cm}^3\,\text{mol}^{-1}$, $\Delta V_a = 8.78\,\text{cm}^3\,\text{mol}^{-1}$, $\Delta V_a = 9.99\,\text{cm}^3\,\text{mol}^{-1}$—for pure 5OCB and nanocolloids, respectively.

When discussing this issue it is worth recalling that for similar studies in 5CB the clearly visible super-Arrhenius relations were reported, at least for the temperature behavior. The case of the clear Arrhenius/Barus behavior for 5OCB may be related to the fact that a 5OCB molecule is ca. 20% longer than a 5CB molecule [11–13].

IV. CONCLUSIONS

Results presented above revealed a set of unique features appearing in dielectric static and dynamic properties when adding nanoparticles to a rodlike liquid crystalline host: in the given case 5OCB and $BaTiO_3$ NPs. First, the ferroelectricity of NPs had a significant influence on results. Second, the superparaelectric phase can exist in NPs below its correlation length, which proved some theoretical considerations and explained, why no differences between cubic and tetragonal-phase NPs influences appeared. Third, the amount of NPs can have a very strong impact on such a basic property, regarding fundamentals, as the discontinuity of the phase transition. It is also notable that patterns observed for temperature and pressure path where different, which in fact could not be revealed for pure LC compounds tested so far. From both the application and the fundamental points of view ithe strong influence of NPs on the value of dielectric constant, activation energy, and FDSE decoupling are important.

ACKNOWLEDGMENTS

The research carried out by was supported via the National Centre for Science (NCN, Poland) Grant No. 2016/21/B/ST3/02203 (S.J.R., A.D.R., S.S.). S.K. acknowledge the financial support from the Slovenian Research Agency (research core funding Grant No. P1-0099).

APPENDIX: PHASE AND STRUCTURAL LIQUID CRYSTAL BEHAVIOR

In the following we illustrate main impacts of NPs on LC behavior in a nanocolloidal sample. We consider mixtures of LC and immersed identical nanoparticles. Quantities characterizing the samples at the mesoscopic level are the volume concentration field of nanoparticles c and the nematic tensor order parameter $\underline{Q}$ describing a local LC orientational ordering. Partially averaged concentration for homogeneously distributed NPs can be expressed as $\overline{c} = N_{NP}v_{NP}/V$. Here N_{NP} represents the number of NPs, v_{NP} describes volume of a nanoparticle, V stands for the volume of the sample, and the overbar $\overline{(\cdots)}$ marks spatial averaging. The corresponding volume concentration of LC molecules in the mixture is $1 - \overline{c}$. We consider cases $\overline{c} \ll 1$; hence, $V \cong V_{LC}$ and V_{LC} stands for the volume occupied by LC molecules. For simplicity, we limit to spherical NPs. Their volume and surface equal $v_{NP} = 4\pi r^3/3$ and $a_{NP} = 4\pi r^2$, respectively, where r stands for the NP radius.

We consider thermotropic LCs that exhibit in bulk the isotropic-nematic phase transition at the critical temperature T_{IM} on varying the temperature T. At the mesoscopic level the orientational LC order is described with the nematic tensor order parameter $\underline{Q}$. In the uniaxial limit it is commonly expressed as $\underline{Q} = s(\vec{n} \otimes \vec{n} - \underline{I}/3)$. The nematic director $\vec{n}$ identifies the local uniaxial ordering direction, the uniaxial

order parameter s measures the extent of fluctuations about this direction, and $\underline{I}$ stands for the identity tensor.

1. Dilution regime

If NPs are negligible coupled with nematic ordering, they act effectively as diluting agents, commonly referred to as *impurities*. For NPs of our interest this is realized if the condition $r/d_e < 1$ is fulfilled, where d_e stands for the surface anchoring extrapolation length. It is defined as $d_e \approx K/W$, where K stands for the representative elastic constant and the constant W measures the anchoring strength. For typical LCs it holds $K \sim 10^{-11}$ J/m^3 and for a moderate anchoring strength $W \sim 10^{-4}$ J/m^2 one gets $d_e \approx 100$ nm.

In the limit $r/d_e \ll 1$ the general thermodynamics well describes the resulting behavior of a mixture. The presence of *impurities* depresses the phase transition temperature $T_{IM}^{(m)}$, where the superscript (m) denotes the mixture. It roughly holds that $T_{IM}^{(m)} \approx RT_{IM}^2(\overline{c}_I - \overline{c}_N)/L_{IN}$, where R is the ideal gas constant, L_{IN} is the molar latent heat of the pure *I-N* transition, and $\{\overline{c}_I,\overline{c}_N\}$ label average concentrations of *impurities* in the coexisting nematic ($\overline{c} = \overline{c}_N$) and isotropic ($\overline{c} = \overline{c}_I$) phases, where $\overline{c}_I > \overline{c}_N$. Furthermore, impurities enhance the temperature window $\Delta T \propto \overline{c}_I - \overline{c}_N$ of the isotropic-nematic phase coexistence.

2. Coupling regime

For cases $r/d_e \geqslant 1$ nanoparticles are sufficiently strong coupled with the nematic ordering to directly influence the local director field. To illustrate the most important effects, we express the free energy of the soft nanocomposite as

$$F = \iiint [f_m + f_c + f_e + f_i\delta(\vec{r} - \vec{r}_i)]d^3\vec{r}, \tag{A1}$$

where δ stands for the δ function, $\vec{r}_i$ locates nanoparticle-LC interfaces, and the integral runs over the LC volume. The mixing (f_m), condensation (f_c), elastic (f_e), and interfacial (f_i) free-energy densities are given by

$$f_m = \frac{k_BT}{v_{NP}}(1-c)\ln(1-c) + \frac{k_BT}{v_{NP}}c\ln c + \kappa c(1-c), \tag{A2}$$

$$f_c = \tfrac{3}{2}A_0(T - T^*)\mathrm{Tr}\underline{Q}^2 - \tfrac{9}{2}B\mathrm{Tr}\underline{Q}^3 + \tfrac{9}{4}C(\mathrm{Tr}\underline{Q}^2)^2, \tag{A3}$$

$$f_e = L\mathrm{Tr}(\nabla\underline{Q})^2, \tag{A4}$$

$$f_i = -\tfrac{3}{2}w_1\vec{v}\cdot\underline{Q}\vec{v} + \tfrac{9}{4}w_2(\vec{v}\cdot\underline{Q}\vec{v}), \tag{A5}$$

where Tr stands for the trace operator. We took into account only the most essential terms which are needed to demonstrate qualitatively different phenomena of our interest. Numerical factors in Eqs. (A3) and (A5) are introduced for latter convenience.

The term f_m describes the isotropic mixing for the two components within the Flory theory, k_B is the Boltzmann constant, v_{LC} measures the volume of a LC molecule, and κ stands for the Flory-Huggins parameter. Note that this parameter promotes phase separation if $\kappa > 0$. Namely, it is minimized for $c = 0$ or $c = 1$, corresponding to "pure" cases.

The condensation term f_c enforces degree of orientational order. The quantities A_0, B, and C are material constants, and T^* describes the supercooling temperature. In bulk equilibrium the phase transition temperature equals $T_{IM} = T^* + B^2/(4A_0C)$, and below T_{IM} the corresponding equilibrium degree of uniaxial ordering is given by $s_{eq} = s_0[3 + \sqrt{9 - 8(t - T^*)/(T_{IM} - T^*)}]/4$, $s_0 = s_{eq}(T_{IM}) = B/(2C)$.

The elastic term f_e is expressed in a single elastic constant approximation and $L > 0$ is the representative bare (i.e., independent of T) elastic constant. This term enforces a spatially homogeneous structure.

The term f_i describes conditions at a LC-NP interface. We included only some symmetry-allowed terms that play important roles in our study. The quantities w_1 and w_2 describe bare surface anchoring strengths, and $\vec{v}$ stands for the local normal vector of an interface.

For convenience we introduce the following characteristic lengths of the system which we express at $T = T_{IM}$: $\xi_{IN}^2 = L/[A_0(T_{IM} - T^*)]$, $d_1 = w_1s_0/(Ls_0^2)$, $d_2 = w_2/L$. Here ξ_{IN} estimates the uniaxial order parameter correlation length, and $\{d_1,d2\}$ stands for surface extrapolation lengths.

a. Phase separation

We next estimate the impact of phase separation on critical behavior in which an orientational ordering is established. To identify main parameters that can trigger phase separation, we describe the system by spatially averaged values $\overline{s}$ and $\overline{c}$. In a phase-separation process regions displaying different values of $\overline{s}$ and $\overline{c}$ are formed. To get insight into key mechanism, we expressed the average free-energy density as $\overline{f} \sim \overline{f}_m + \overline{f}_c + \overline{f}_e + \overline{f}_i$, where

$$\overline{f}_m \sim \frac{4k_BT}{v_{LC}}(1-\overline{c})\ln(1-\overline{c}) + \frac{4k_BT}{v_{NP}}\overline{c}\ln\overline{c} + \kappa\overline{c}(1-\overline{c}), \tag{A6}$$

$$\overline{f}_c = (1-\overline{c})\left[A_0(T - T^*)\overline{s}^2 - B\overline{s}^3 + C\overline{s}^4\right], \tag{A7}$$

$$\overline{f}_e \sim (1-\overline{c})\frac{L\overline{s}^2}{\xi_d^2}, \tag{A8}$$

$$\overline{f}_i \sim \overline{c}(1-\overline{c})(-w_1\overline{s} + w_2\overline{s}^2)\frac{r}{4}. \tag{A9}$$

To understand phase separation tendencies of our system, it is convenient to introduce the effective Flory-Huggins parameter κ_{eff} as the coefficient weighting the contribution proportional to $\overline{c}(1-\overline{c})$ in $\overline{f}$; i.e.,

$$\kappa_{\mathrm{eff}} = \kappa + A_0\lambda\overline{s}^2 - \frac{a_{NP}}{v_{NP}}w_1\overline{s} + \frac{a_{NP}}{v_{NP}}w_2\overline{s}^2. \tag{A10}$$

If κ_{eff} is larger than its critical value, $\kappa_c > 0$, it triggers phase separation. Namely, its contribution in free-energy expression is minimal for $\overline{c} = 0$ or $\overline{c} = 1$. For common LCs it holds true that $\kappa \ll A_0\lambda\overline{s}^2$ and $\kappa < \kappa_c$, and we assume that this is realized in samples of our interest. Let us first neglect the surface interaction term contributions. Therefore, mixture is homogeneous in the absence of orientational ordering and on entering the nematic phase κ_{eff} strongly increases due to the established ordering, which very likely triggers phase

separation, leading to the coexistence regime. Furthermore, surface interaction could either enhance or suppress the phase separation tendency. In most samples w_1 and w_2 are positive, and consequently the w_1 (w_2) contribution tends to suppress (enhance) phase transition tendency. Therefore, surface treatment could strongly affect phase separation tendency.

b. Nematic structural behavior

We next estimate the impact of NPs on LC orientational ordering across the phase transition region for relatively low concentrations $\bar{c}$, neglecting phase separation. We approximate the free energy $\overline{F}$ of the system by the expression

$$\overline{F} = \left\{\left[A_0(T-T^*) + \frac{L}{\xi_d^2}\right]\bar{s}^2 - B\bar{s}^3 + C\bar{s}^4\right\}V + (-\bar{s}w_1 + \bar{s}^2 w_2)N_{NP}a_{NP}. \tag{A11}$$

In expressing Eq. (A11) we estimate average NP-induced elastic distortions by $|\overline{\nabla\vec{n}}| \sim 1/\xi_d$, where we assumed mono domain-type structure in the nematic director pattern.

For analytical transparency reasons we introduce the scaled order parameters $\tilde{s} = \bar{s}/s_0$, the dimensionless temperature $t = (T-T^*)/(T_{IM}-T^*)$, and dimensionless free-energy density $\tilde{f} = \overline{F}/[VA_0(T_{IM}-T^*)s_0^2]$. In the following we omit the tildes to avoid clutter and it follows that

$$f = t^{(\mathrm{eff})}s^2 - 2s^3 + s^4 - \sigma s, \tag{A12}$$

where $t^{(\mathrm{eff})} = t + \xi_{IN}^2/\xi_d^2 + (w_2/|w_2|)\bar{c}3\xi_{IN}^2/(d_2 r)$ and $\sigma = (w_1/|w_1|)\bar{c}\xi_{IN}^2/(d_1 r)$.

The phase behavior of the system described by Eq. (A12) is as follows. For $\sigma < \sigma_c \equiv 0.5$ the first-order phase transition takes place when the condition $t^{(\mathrm{eff})} = t_c^{(\mathrm{eff})} \equiv 1+\sigma$ is realized. The corresponding critical temperature shift $\Delta T = T_{IM}^{(m)} - T_{IM}$ reads

$$\frac{\Delta T}{T_{IM}-T^*} = \frac{w_1}{|w_1|}\frac{\bar{c}3\xi_{IN}^2}{d_2 r} - \frac{\xi_{IN}^2}{\xi_d^2}. \tag{A13}$$

Therefore, $w_1 > 0$ (surface ordering potential) tends to increase $T_{IM}^{(m)}$, while $w_2 > 0$ (surface disordering potential) and elastic distortions suppress $T_{IM}^{(m)}$. Above the phase transition the isotropic ordering is replaced by finite paranematic degree of ordering. For $\sigma > \sigma_c$ the supercritical regime is entered where on decreasing temperature the average nematic order parameter gradually increases.

Note that, in general, NPs enforce a relatively complex distortion to surrounding LC ordering in the case of finite anchoring strengths at NP-LC interfaces. They might even trigger formation of topological defects due to energetic or even topological reasons. However, studies reveal that the distortions are within a reasonable approximation presented by a single characteristic length [23–27], which is in our treatment characterized by the average domain length ξ_d [see Eq. (A8)]. Therefore, geometrical details (i.e., shape of NPs, easy anchoring directions) enter our model via ξ_d. There were several theoretical studies [23,28–33] in which ξ_d was treated as a variational parameter. However, the key qualitative features (phase separation tendency, phase temperature shifts, vanishing of a phase transition) are captured by our simple minimal model. For example, a single characteristic domain length is, in the case of a weak enough disorder (enabled by NPs), predicted by the universal Imry-Ma theorem [23,33]. It applies to any continuous symmetry-breaking phase transition in the presence of a random field-type distortion. According to it, the domain length is estimated by $\xi_d \sim w^{-2/(4-d)}$. Here w measures the disorder strength, and d is the dimensionality of space.

c. Impact of disorder

In our experiments one observes decreased values of dielectric strength in the pretransitional regime for relatively low concentrations of NPs. It is very likely that NP-induced disorder plays a dominant role.

To demonstrate its origin, we assume that locally the NP-LC interface tends to increase nematic ordering (i.e., the term weighted by $w_1 > 0$ dominates at the interface). Consequently, NPs nucleate clusters of size ξ_d exhibiting paranematic ordering. In the low-concentration limit it holds $\xi_d \approx \xi$. Here $\xi(T)$ stands for the nematic order parameter correlation length, which is maximal at T_{IM}, where $\xi(T_{IM}) = \xi_{IN}$. If $l_{NP} \sim (v_{NP}/\bar{c})^{1/3} > \xi_d$, where l_{NP} estimates the average separation among NPs, then bulklike behavior is expected.

Note that for $l_{NP} \geqslant \xi_d$ paranematic preferential alignment in different clusters is weakly correlated. Furthermore, on approaching the phase transition, on decreasing T, fluctuation-enabled clusters exhibiting nematic ordering become more abundant, and they tend to expel *impurities* (i.e., NPs) into the less ordered surrounding region. Consequently, concentration of impurities increases in paranematic regions, lowering a local value of l_{NP}. Because fluctuations are strong in these regimes, one expects relatively broader distribution of ξ_d values with respect to pure sample. In regimes where $l_{NP} \sim \xi_d$, different clusters interact and, in general, experience frustration if their average symmetry-breaking directions are significantly different, leading to substantial increase in disorder.

On still increasing $\bar{c}$, nearby clusters become more coupled and correlated, which decreases degree of ordering.

[1] S. J. Rzoska, S. Starzonek, A. Drozd-Rzoska, K. Czupryński, K. Chmiel, G. Gaura, A. Michulec, B. Szczypek, and W. Walas, Phys. Rev. E **93**, 020701 (2016).

[2] P. K. Mukherjee, Europhys. Lett. **114**, 56002 (2016).

[3] P. K. Mukherjee, J. Mol. Liq. **225**, 462 (2017).

[4] S. J. Rzoska, S. Starzonek, and A. Drozd Rzoska, in *Advances in Colloid Science*, edited by M. M. Rahman and A. M. Asiri (InTech, Rijeka, Croatia, 2016), p. 265.

[5] S. Kralj, Z. Bradač, and V. Popa-Nita, J. Phys.: Condens. Matter **20**, 244112 (2008).

[6] L. M. Lopatina and J. V. Selinger, Phys. Rev. E **84**, 041703 (2011).

[7] L. M. Lopatina and J. V. Selinger, Phys. Rev. Lett. **102**, 197802 (2009).

[8] Q. Li, *Liquid Crystals Beyond Displays: Chemistry, Physics and Application* (Wiley, New York, 2012).

[9] G. Vertogen and W. H. de Jeu, *Thermotropic Liquid Crystals-Fundamentals*, Springer Series in Chemical Physics (Springer, Berlin, 2008).
[10] P. G. de Gennes, *The Physics of Liquid Crystal* (Oxford University Press, Oxford, UK, 1974).
[11] P. K. Mukherjee, S. J. Rzoska, and A. Drozd-Rzoska, *Linear and Nonlinear Dielectric Insight into the Isotropic Phase of Liquid Crystalline Materials* (Lambert, Saarbruecken, 2015).
[12] A. Drozd-Rzoska, S. J. Rzoska, and J. Zioło, Phys. Rev. E **54**, 6452 (1996).
[13] A. Drozd-Rzoska, S. Rzoska, and K. Czupryñski, Phys. Rev. E **61**, 5355 (2000).
[14] A. Drozd-Rzoska, S. J. Rzoska, and J. Zioło, Phys. Rev. E **61**, 5349 (2000).
[15] A. Drozd-Rzoska, S. Rzoska, S. Pawlus, and J. Zioło, Phys. Rev. E **72**, 031501 (2005).
[16] G. S. Iannacchione, C. W. Garland, J. T. Mang, and T. P. Rieker, Phys. Rev. E **58**, 5966 (1998).
[17] A. Roshi, G. S. Iannacchione, P. S. Clegg, and R. J. Birgeneau, Phys. Rev. E **69**, 031703 (2004).
[18] S. Pawlus, J. Osinska, S. J. Rzoska, S. Kralj, and G. Cordoyiannis, in *Soft Matter Under Exogenic Impacts*, edited by S. J. Rzoska and V. A. Mazur (Springer, Netherlands, 2007), p. 229.
[19] M. D. Glinchuk, E. A. Eliseev, and A. N. Morozovska, Phys. Rev. B **78**, 134107 (2008).
[20] S. J. Rzoska, A. Drozd-Rzoska, P. K. Mukherjee, D. O. Lopez, and J. C. Martinez-Garcia, J. Phys.: Condens. Matter **25**, 245105 (2013).
[21] L. Mistura, J. Chem. Phys. **59**, 4563 (1973).
[22] S. Starzonek, S. J. Rzoska, A. Drozd-Rzoska, S. Pawlus, E. Biała, J. C. Martinez-Garciac, and L. Kistersky, Soft Matter **11**, 5554 (2015).
[23] Y. Imry and S.-k. Ma, Phys. Rev. Lett. **35**, 1399 (1975).
[24] D. J. Cleaver, S. Kralj, T. J. Sluckin, and M. P. Allen, in *Liquid Crystals in Complex Geometries Formed by Polymer and Porous Networks*, edited by G. P. Crawford and S. Zumer (Taylor & Francis, London, 1996), p. 467.
[25] T. Bellini, M. Buscaglia, C. Chiccoli, F. Mantegazza, P. Pasini, and C. Zannoni, Phys. Rev. Lett. **85**, 1008 (2000).
[26] T. Bellini, L. Radzihovsky, J. Toner, and N. A. Clark, Science **294**, 1074 (2001).
[27] M. Buscaglia, T. Bellini, C. Chiccoli, F. Mantegazza, P. Pasini, M. Rotunno, and C. Zannoni, Phys. Rev. E **74**, 011706 (2006).
[28] V. Popa-Nita, Eur. Phys. J. B **12**, 83 (1999).
[29] V. Popa-Nita and S. Romano, Chem. Phys. **264**, 91 (2001).
[30] S. Kralj and V. Popa-Nita, Eur. Phys. J. E **14**, 115 (2004).
[31] A. Ranjkesh, M. Ambrožič, S. Kralj, and T. J. Sluckin, Phys. Rev. E **89**, 022504 (2014).
[32] B. Takabi and M. Alizadeh, *Nanofluid and Hybrid Nanofluid* (Lambert, New York, 2014).
[33] Y. Imry and M. Wortis, Phys. Rev. B **19**, 3580 (1979).